frontiers | Frontiers in Materials

TYPE Original Research
PUBLISHED 03 October 2022
DOI 10.3389/fmats.2022.999753

OPEN ACCESS

EDITED BY
Dawei Wang,
Shenzhen Institutes of Advanced Technology (CAS), China

REVIEWED BY
Peng He,
Anhui Polytechnic University, China
Junying Zhang,
Beijing University of Chemical Technology, China
Weili Song,
Beijing Institute of Technology, China

*CORRESPONDENCE
Genliang Hou,
hougenliang@163.com
Song Bi,
xiaozhu-youyou@163.com

SPECIALTY SECTION
This article was submitted to Ceramics and Glass, a section of the journal Frontiers in Materials

RECEIVED 21 July 2022
ACCEPTED 14 September 2022
PUBLISHED 03 October 2022

CITATION
Li H, Hou G, Yuan X, Liu Z, Luo W, Song Y and Bi S (2022), KOH modification of fluorinated graphite and its reaction mechanism.
Front. Mater. 9:999753.
doi: 10.3389/fmats.2022.999753

KOH modification of fluorinated graphite and its reaction mechanism

Hao Li[1], Genliang Hou[1]*, Xiaojing Yuan[1], Zhaohui Liu[2], Weipeng Luo[1], Yongzhi Song[1] and Song Bi[1]*

[1]304 Department, Xi'an Research Institute of High-Tech, Xi'an, Shaanxi, China, [2]College of Weapon Science and Technology, Xi'an Technological University, Xi'an, Shaanxi, China

KOH electrochemical method and heating method were employed to modify fluorinated graphite and explore the modification mechanism. The chemical composition and microstructure of the products were characterized and analyzed before and after the reaction. As the electrochemical reaction time or heating temperature increased, the carbon fluorine bond gradually underwent a nucleophilic reaction with KOH according to its reactivity, promoting the formation of fluorine ions in the residual product and carbon oxygen bonds in the corresponding oxidized fluorinated graphite (OFG). The electrochemical method with the anode on the bottom and the heating method were insufficient to allow the isolated carbon fluorine bond to react, retaining some carbon fluorine bonds. By positioning the anode on top, electron transfer significantly accelerates the activation of the carbon fluorine bond, which then reacts completely. According to theoretical simulation calculations, electronegative groups around the carbon fluorine bond can effectively enhance its reactivity.

KEYWORDS

oxidized fluorinated graphite, KOH modification, nucleophilic reaction, electrochemical reaction, carbon-fluorine bond activation

1 Introduction

Graphene grafted with fluorine atoms and oxygen-containing groups is known as oxidized fluorinated graphite (OFG). OFG is comprised of both fluorinated graphene (FG) and graphene oxide (GO) in structure, which is reflected in its demonstrated performance (Chen et al., 2021). The properties of OFG, such as its hydrophilicity (Zhu et al., 2019), lubricity (Ma et al., 2021), insulating ability (Xu et al., 2021) and photoelectric performance (Gong et al., 2018), can be significantly adjusted by varying its content of F and O.

Owing to its unique performance, OFG is widely used in hydrophobic coatings (Zhao et al., 2021), sensors (Yeon-Hoo et al., 2017), medicine (Razaghi et al., 2020), lithium batteries (Kaczmarek et al., 2021) and many other applications. According to the raw materials used, there are two main approaches to the preparation of OFG. One is to use GO as a raw material and use HF, XeF_2 or HPF_6 as fluorinating agents to obtain OFG

(Jahanshahi et al., 2020; Yamamoto et al., 2020; Sim et al., 2022). OFG was synthesized *via* plasma discharge in a dielectric barrier (DBD) plasma reactor, taking NF_3 as the F-radical-generating gas, and H_2 catalysed the dissociation of NF_3 (Sim et al., 2022). GO can be fluorinated by SF_4 to obtain OFG below the decomposition temperature of GO (~200°C) under the catalysis of HF (Yamamoto et al., 2020). OFG was also prepared at mild temperature (80°C) by using ammonium fluoride salt as fluorine agent and a synthesized acidic IL ($[TEA]^+[TFA]^-$) as a solvent (Jahanshahi et al., 2020). Another approach is to prepare OFG using fluorinated graphite (FGi) as a raw material *via* oxygen doping (Fan et al., 2017; Guguloth et al., 2021; Li et al., 2022). FGi (F/C = 1) in DMF solution was also heated to prepare OFG (Fan et al., 2017). OFG with different fluorine and oxygen content was synthesized by using the Hummers method to oxidize the $(CF_{0.46})_n$ (Li et al., 2022). In addition, the electrochemical oxidation of graphite in HF solution can also obtain OFG (Matsuo et al., 2016).

In addition, FGi is superposed by FG. Theoretical calculations have suggested that FG is vulnerable to S_N2 nucleophilic attack and can be used as a precursor to other graphene derivatives (Matúš et al., 2015). FG can be nucleophilically substituted by amines (Siedle et al., 2021) and hydroxyl groups (Kouloumpis et al., 2020) or reduced by hydrazine (Robinson et al., 2010), KI (Borse et al., 2022), and Zn (Liang et al., 2017), etc. Therefore, FGi can be nucleophilically substituted by hydroxyl groups to synthesize OFG with hydroxyl. A 180°C molten KOH and NaOH mixture was used to modify FGi to obtain OFG quantum dots (about 3 nm), which have a stable fluorescence and can be applied at different pH (Gong et al., 2015). A mixture of NaOH/KOH and FGi was heated at 250°C for 8 h to obtain graphitized carbon particles (Bourlinos Athanasios et al., 2008). However, the high-temperature molten alkali makes it difficult to control the fluorine and oxygen content of OFG.

As previously reported, there are two main methods for preparing OFG (Fan et al., 2017; Jahanshahi et al., 2020; Yamamoto et al., 2020; Guguloth et al., 2021; Li et al., 2022; Sim et al., 2022). However, it is still difficult to control the contents and types of fluorine and oxygen. Oxygen-containing groups can be somewhat controlled by modifying FG with OH^-; however, there are still two problems. First, it is difficult to control the oxygen content due to the violent reaction between the molten alkali and FGi, which causes FGi to lose nearly all fluorine (Gong et al., 2015). Second, the reaction mechanism of this process is unclear (Bourlinos Athanasios et al., 2008). In view of this, KOH heating or electrolysis in an organic solvent was adopted to avoid severe damage to FGi from the high-temperature molten alkali. In addition, the reaction processes and products were studied in detail to elucidate the reaction mechanism.

2 Experimental section

2.1 Materials preparation

FGi with fluorine/carbon ratios of ~0.46, ~0.95, and ~1.17 were provided by Shanghai CarFluor Ltd. and respectively termed $CF_{0.46}$, $CF_{0.95}$, and $CF_{1.17}$. Potassium hydroxide, methanol, and ethanol were provided by Sinopharm Chemical Reagent Co., Ltd. Deionized water (>18 MΩ cm) was used for the rinsing and as the solvent.

2.2 Synthesis of oxidized fluorinated graphite

Considering that only water and carbon dioxide or carbonate are formed from methanol electrolysis and no organic products are generated, methanol was selected as the solvent for electrolysis (Menia et al., 2017). Because methanol has a low boiling point, ethanol was used instead in the heating method.

KOH electrochemical method in methanol: First, 8 g KOH was dissolved in 60 ml methanol by stirring. 0.5 g $CF_{1.17}$ was added, and the mixture was stirred for 5 min to ensure uniform dispersion. The mixture was poured into a tapered, bottomed vertical glass cylinder with an inner diameter of 25 mm (Figure 10). Both the anode and cathode were made of Pt wire. With the anode at the top, the solution was electrolyzed at 60 V DC for 2 h, 5 h and until there was no current, during which methanol was continuously added to keep the volume of the solution unchanged. After the final solution was poured into a beaker and ultrasonically dispersed for 30 min in water to uniformize it and facilitate stripping. After filtration, the solid was freeze-dried in water for 48 h and then dried at 100°C for 12 h to obtain the final product, OFG1.17-E2, OFG1.17-E5, and OFG1.17-E00, respectively. OFG1.17-E01 was obtained by changing the anode of OFG1.17-E00 to the bottom and keeping the other conditions the same.

KOH heating method in ethanol: First, 8 g KOH was dissolved in 60 ml methanol by stirring. Then, 0.5 g $CF_{1.17}$ was added, and the mixture was stirred for 5 min to make uniform dispersion. The solution in the sealed beaker was stirred for 24 h at 20°C, then added to water, and freeze-dried for 48 h, and finally dried at 100°C for 12 h to obtain the final product, OFG1.17-H20. The corresponding products at 40°C, 60°C, 80°C and 100°C were recorded as OFG1.17-H40, OFG1.17-H60, OFG1.17-H80, and OFG1.17-H100 respectively. The corresponding products of different modification methods are summarized in Table 1.

TABLE 1 Corresponding products of different modification method.

Raw material	Modification method	Reaction condition	Products	Residual products
$CF_{1.17}$ (0.5 g)	electrochemical method	60 V 2 h	OFG1.17-E2	RP1.17-E2
KOH (6 g)				
CH_3OH (60 ml)		60 V 5 h	OFG1.17-E5	RP1.17-E5
		60 V until no current	OFG1.17-E00	RP1.17-E00
		60 V until no current with the bottom anode	OFG1.17-E01	RP1.17-E01
$CF_{1.17}$ (0.5 g)	heating method	20°C	OFG1.17-H20	RP1.17-H20
KOH (6 g)				
C_2H_5OH (60 ml)		40°C	OFG1.17-H40	RP1.17-H40
		60°C	OFG1.17-H60	RP1.17-H60
		80°C	OFG1.17-H80	RP1.17-H80
		100°C	OFG1.17-H100	RP1.17-H100

2.3 Separation and extraction of residual products

The chemical components of OFG and the residual products were analyzed in detail to study the reaction mechanism of the modification of FGi with different fluorine contents by KOH. After OFG was separated by suction filtration, the remaining solution was dried at 140°C for at least 48 h, and the product was recorded as the residual product (RP). For example, RP1.17-E2 corresponded to the residual product of OFG1.17-E2. RP1.17-E2 was diluted to 1 mg/ml with water for determining the fluorine ion concentration using ion chromatography. Fluorine ion concentration multiplied by RP1.17-E2 mass (in mg) is the mass of fluorine ion.

2.4 Characterization

Fourier transform infrared (FT-IR) spectroscopy from 400 cm^{-1} to 4,000 cm^{-1} was recorded by using a VERTEX70 spectrometer (Bruker, Germany). X-ray photoelectron spectroscopy (XPS) analysis was performed using an X-ray photoelectron spectrometer (Thermo Fisher Scientific, United States) with a monochromatic Al Kα (1486.6 eV) line. All binding energies were calibrated using the 284.6 eV binding energy of C 1s. The crystal structure was characterized by X-ray diffraction (XRD) using an excitation source of the Ka line of the Cu target (λ = 0.154 nm) (X'Pert PRO, PANalytical, Netherlands). The micromorphology was observed using a Tecnai G2 F20 transmission electron microscope (TEM, FEI, United States), and the samples were ultrasonically dispersed on a pure carbon film. The distribution of elements was measured using an Oxford 80T energy-dispersive X-ray spectrometer (EDX, Oxford, United Kingdom) instrument equipped with a TEM. The F ion concentration was determined by ion chromatography (Thermo Fisher, ICS-1000 type, United States).

3 Results and discussion

Due to the small radius and high electronegativity of fluorine, the carbon fluorine bond has a high degree of polarization, making it the strongest carbon atom single bond. Although the C-F bond has a very high bond energy, its polarity is very high, which makes it break easily (Matúš et al., 2015). Consequently, F can instead be replaced by nucleophile, but the selectivity of the nucleophilic substitution reaction remains a great challenge. KOH was thus utilized to react FGi by controlling the reaction conditions.

3.1 Morphology and chemical composition of OFG

3.1.1 KOH electrolytic method in methanol solution

FGi was electrolyzed in a KOH methanol solution and the effect of FGi modification was studied by controlling the reaction time and other conditions.

Table 2 shows the contents of C, O and F in OFG1.17-E. Compared to $CF_{1.17}$, OFG1.17-E exhibits obvious changes, especially OFG1.17-E00 and OFG1.17-E01 following complete electrolysis. The O content of OFG1.17 gradually increases with the electrolysis time, while the F content decreases. In the FT-IR spectrum, peaks corresponding to oxygen-containing groups (the–OH vibration peaks near 3,438 cm^{-1} and the C–O vibration peaks at around 1041 cm^{-1}) (Zhang et al., 2021) began to appear, and the characteristic peaks for C–F and–CF_2 (1345 and 1190 cm^{-1}, respectively) gradually disappeared (Supplementary Figure S1A). Notably, the O

TABLE 2 Elemental contents of OFG1.17-E.

Products	C (at%)	O (at%)	F (at%)	Others (at%)
$CF_{1.17}$	45.1	0.6	54.3	
OFG1.17-E2	44.6	2.3	52.6	Si 0.5
OFG1.17-E5	45.8	2.7	51.5	
OFG1.17-E00	69.7	21.8	1.7	Na 0.4, K 4.4, Si 2.0
OFG1.17-E01	64.5	20.0	11.4	Na 0.5, K 2.5, Si 1.1

anode. The C-O bond of OFG1.17 may be derived from the nucleophilic reaction between KOH and the C-F bond in graphite fluoride (He et al., 2019). The C-O bond content of OFG1.17-E2 and OFG1.17-E5 is much lower than that of OFG1.17-E00 and OFG1.17-E01, indicating that the nucleophilic reaction of the carbon–fluorine bond with KOH occurred more readily over time. In addition, the formation of carbon oxygen bonds is not consistent with the breakage of carbon fluorine bonds, with a large number of carbon fluorine

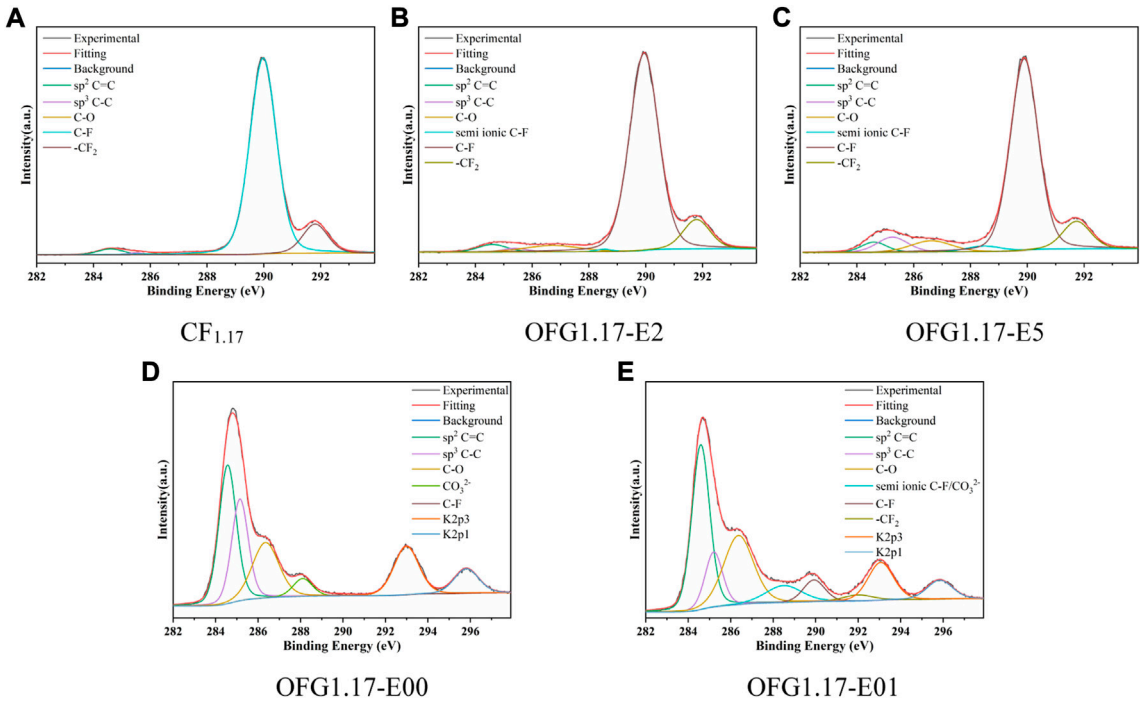

FIGURE 1
High-resolution C1s spectra of OFG1.17-E: E2(2 h), E5(5 h), E00(no current), and E01(bottom anode).

contents of OFG1.17-E00 and OFG1.17-E01 are basically consistent. However, the F content of OFG1.17-E00 is only 1.74 at%, while that of OFG1.17-E01 is 11.4 at%, indicating that the position of the anode has a great influence. Furthermore, the existence of trace amounts of Na, K and Si result from the reaction of KOH with the glass container. The elemental distribution of OFG1.17-E is uniform after KOH electrochemical modification, especially for F and O (Supplementary Figure S2 in the Supporting Information).

The high-resolution C1s spectra of OFG1.17-E (Figure 1) shows the amount of carbon oxygen bonds gradually increase with the electrolysis time, containing mostly C-O bonds (286.5 eV), no C=O bond (287.8 eV) and few possible O-C=O bonds (288.5 eV). C-O is not further oxidized despite the presence of an electrochemical oxidation potential on the bonds being converted to carbon-carbon bonds. A likely explanation is that KOH undergoes a nucleophilic reaction with the carbon fluorine bond, but the condensation reaction of carbon oxygen bonds reduces the oxygen content and leads to the formation of carbon-carbon bonds. The XRD spectrum and actual photo (Supplementary Figure S3, S4 in the Supporting Information) also indirectly show the destruction of the carbon fluorine bond structure.

According to the above analysis, an increased electrolysis time can promote the nucleophilic reaction, causing the C-O bond content to increase proportionally. KOH will not immediately destroy the carbon fluorine bond, but electrolysis for extended periods will cause substantial damage to the carbon fluorine bond, and the anode position has an important impact on the fluorine content.

TABLE 3 Elemental contents of OFG1.17-H.

Products	C (at%)	O (at%)	F (at%)	Others (at%)
$CF_{1.17}$	45.1	0.6	54.3	
OFG1.17-H20	47.0	2.0	50.1	K 0.2
OFG1.17-H40	46.8	2.5	49.7	K 0.4
OFG1.17-H60	49.8	4.2	43.9	K 1.5
OFG1.17-H80	71.3	17.1	7.1	K 3.9
OFG1.17-H100	72.5	18.4	2.9	K 3.9, N 1.8

3.1.2 KOH heating method in ethanol solution

To further explore the reaction mechanism between KOH and FGi, besides the electrochemical method, a heating method in a KOH ethanol solution was also used for the modification of $CF_{1.17}$. The influence of different temperatures was studied, and the corresponding products obtained at 20°C, 40°C, 60°C, 80°C and 100°C were recorded as OFG1.17-H20 to OFG1.17-H100.

Table 3 shows the contents of C, O and F of OFG1.17-H. With an increase in temperature, the O content increases gradually, while the F content decreases. This was verified by the appearance of -OH (3,438 cm^{-1} and 1626 cm^{-1}) and C-O (1041 cm^{-1}) groups and the disappearance of the C-F (1215 cm^{-1}) and -CF_2 (1319 cm^{-1}) bonds (Supplementary Figure S5A). When the temperature is lower than 60°C, there is a small increase in O content, retaining a high fluorine content. Once the temperature exceeds 80°C, the F content decreases rapidly, and the O content also increases. However, the increase in O content is far less than the decrease in F content. K detected originates from residual KOH. According to the above information, at temperatures over 80°C, KOH will react with $CF_{1.17}$ in large quantities, and the sum of F and O contents is not consistent, indicating that only some KOH undergoes nucleophilic reaction with carbon fluorine bonds. The distributions of F and O elements are basically the same as those of C (Supplementary Figure S6 in the Supporting Information).

Figure 2 shows the C1s peaks of OFG1.17 obtained by the heating method. The carbon fluorine bond content decreases with increasing temperature (from OFG1.17-H20 to OFG1.17-H100), while the carbon oxygen bond content increases gradually, similar to the unsaturated carbon bond content. The increase in carbon-carbon bonds indicates that not all carbon fluorine bonds are changed to carbon oxygen bonds, which may be due to the reduction in carbon oxygen bonds resulting from the condensation reaction of the geminal and vicinal diols. A large number of π-π * bonds (291.7 eV) forms, and -CF_3 (292.6 eV) peak appears at 80°C, which originates from the fracture and detachment of the carbon skeleton, resulting in the formation of -CF_3 and many semi-ionic C-F bonds (288.7 eV). At 100°C, the content of carbon fluorine bonds decreases to 5% (Supplementary Table S2). In addition, the dehydration and condensation of glycol may also result in the formation of C=O and O-C=O.

In the KOH heating method, fewer nucleophilic reactions occurring below 60°C and more nucleophilic reactions at temperatures above 80°C will cause -OH to replace F. However, in this process, only one part of the carbon fluorine bond becomes a carbon oxygen bond, with the other becoming a carbon-carbon bond.

Whether KOH electrochemical method or heating method is used, the oxygen content of OFG increases gradually with the increase in time or temperature. However, the oxygen and fluorine contents of the final products differ slightly. Similar to $CF_{1.17}$, the reaction products of $CF_{0.95}$ and $CF_{0.46}$ are analyzed in the Supporting Information. According to Supplementary Figure S9–S16; Supplementary Table S3–S7, $CF_{0.95}$ and $CF_{0.46}$ also undergo different degrees of nucleophilic reaction with KOH, with lower carbon oxygen bond content.

3.2 Chemical composition of the residual products

From the above analysis, the fluorine content of OFG1.17 is lower than that of $CF_{1.17}$. To confirm the trace of decreasing fluorine content, the chemical compositions of the residual products were analyzed, with the focus on the fluorine content.

The F1s peaks of RP1.17-E (Figure 3) indicate that F1s contains fluorine ion bond peaks (684.8 eV) and the fully electrolyzed RP1.17-E00 and RP1.17-E01 also own the hydrated fluorine ion peaks (682.9 eV), which exist essentially in the form of F ions. The F ion bond originates from the breakdown of the C-F covalent bond in FGi under the nucleophilic influence of KOH, and the F ion cannot form the fluorosilicate in a strong alkaline environment, so there is no fluorosilicate. The strength of the F1s peak increases significantly with increasing reaction time, indicating that the amount of F ions increases.

The F1s peaks of RP1.17-H are shown in Figure 4. Similar to the electrochemical method, all RP1.17-E contain hydrated F ion bonds (683.0 eV), and F ion bonds (684.8 eV) exists in RP1.17-H80 and RP1.17-H100 at higher reaction temperatures. Below 60°C, the peak strength of hydrated F ions increases gradually with the temperature, but this change is less noticeable at temperatures above 60°C. The KOH electrochemical method can only form an F ion bond when the time is sufficient, showing that the hydration ion forms more readily when the F ion content is low. In addition, drying at 140°C for 48 h is not enough to remove KF crystal water. The strength of the F1s peak increased significantly with an increase in the reaction temperature, indicating an increase in the content of the F ions.

Similar to $CF_{1.17}$, all the remaining products of $CF_{0.95}$ and $CF_{0.46}$ modified by KOH contain a low content of fluorine ions (Supplementary Figure S17–S20; Supplementary Table S8–S11).

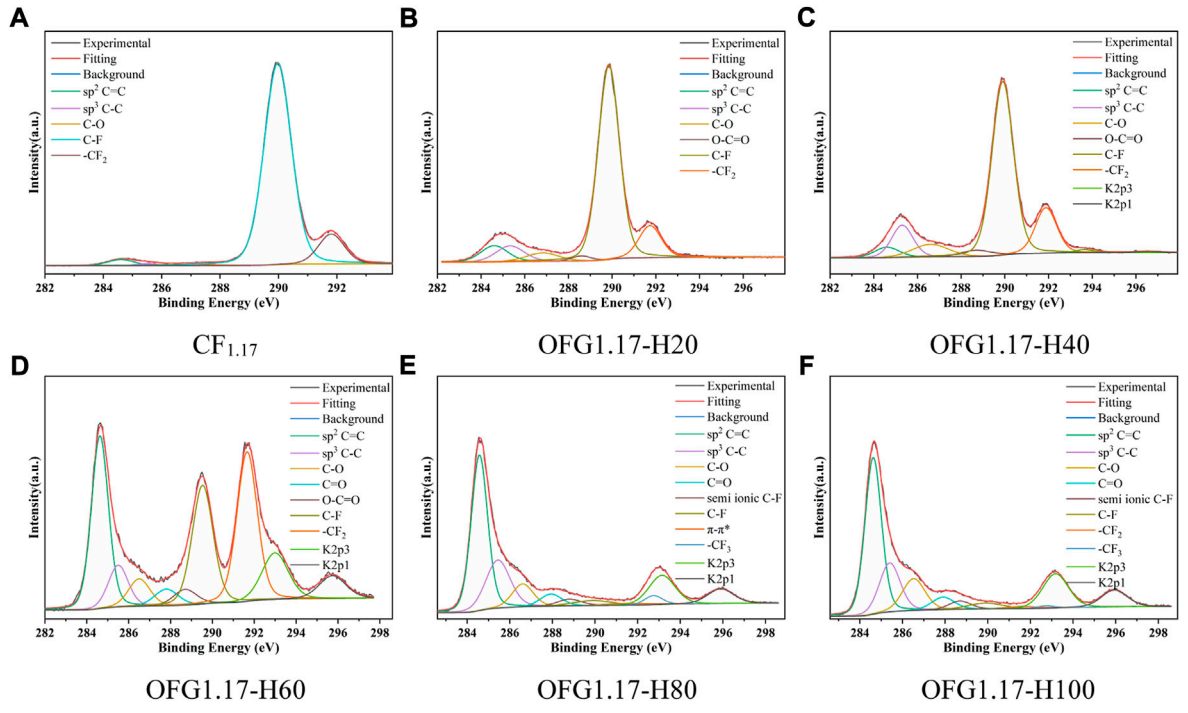

FIGURE 2
High-resolution C1s spectra of OFG1.17-H: H20(20°C), H40(40°C), H60(60°C), H80(80°C), and H100(100°C).

As the reaction time or the temperature increases, the F ion content in the residual product increases, while the fluorine content in the corresponding OFG is gradually decreased.

3.3 Reaction mechanism

Table S1S2 shows the proportion of carbon-carbon bonds (sp^2 C=C and sp^3 C-C), carbon oxygen bonds (C-O, C=O and O-C=O) (He et al., 2019; He et al., 2022), and carbon fluorine bonds (semi-ion C-F, C-F and -CF_2) (Li et al., 2016) in OFG1.17. The amount of carbon-oxygen bonds increased gradually with the reaction time (from OFG1.17-E2 to OFG1.17-E00), but carbon fluorine bonds almost entirely disappear. The position of the anode makes the carbon fluorine bond content of OFG1.17-E01 significantly higher than that of OFG1.17-E00. Similarly, the carbon oxygen bond content decreases obviously with decreasing temperature (from OFG1.17-H20 to OFG1.17-H100), and the rangeability is not consistent with that of carbon fluorine bonds; not all carbon fluorine bonds are converted to carbon oxygen bonds. The F ion bonds in the remaining products of KOH modification indicate that the carbon fluorine covalent bond of $CF_{1.17}$ has been destroyed and converted to fluorine ionic bond. Table 4 shows the F ion content in RP1.17, as determined by ion chromatography and the F concentration in OFG1.17, as determined by XPS. With the increase in electrolysis time or temperature, the number of F ions increase significantly. Considering the experimental error, the F ion content of RP1.17 and the F content of OFG1.17 are basically consistent with the original F element content of $CF_{1.17}$, indicating that no other fluorine-containing substances are generated.

Keith suggests that a typical C-F bond is so strong that the nucleophilic reaction is difficult. However, the C-F bond energy on the graphene skeleton is weakened, reducing the energy barrier for the nucleophilic reactions (Whitener et al., 2015). FGi was modified by -NH_2 (Hou et al., 2014; Bosch-navarro et al., 2015; Ye et al., 2016), -SH (Veronika et al., 2015), the Grignard reagent (Chronopoulos Demetrios et al., 2017), KOH or NaOH (Zhang et al., 2016), respectively, which shows that the carbon fluorine bond of FGi can indeed undergo nucleophilic reactions. Furthermore, there are some differences between the electrochemical and the heating methods. Generally, the carbon fluorine bond of organic fluorides is inert. However, under the condition of electroreduction, the fracture of the carbon fluorine bond connected to an aromatic or alkenyl group is relatively easy because the ability of the π-electron system to accept electrons plays an important role in the subsequent process. The reaction activity and mechanism of the carbon fluorine bond in trifluoromethyl aromatic hydrocarbons (benzyl fluoride) under the electroreduction condition has been studied (Andrieux et al., 1997), indicating that the double electron reduction of trifluoromethyl aromatic

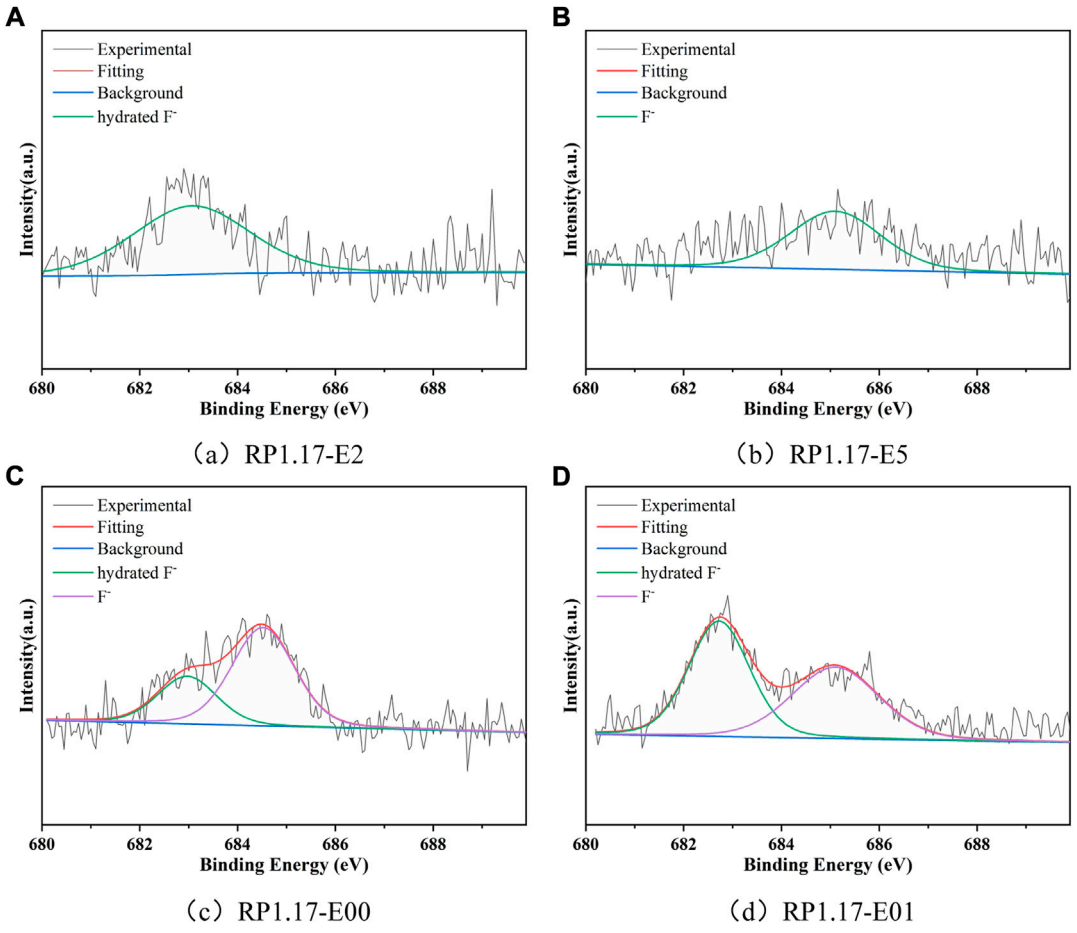

FIGURE 3
High-resolution F1s spectra of RP1.17-E: E2(2 h), E5(5 h), E00(no current), and E01(bottom anode).

hydrocarbons generates fluorine ions and corresponding carbon anion intermediates that can be captured by electrophilic reagents.

According to the reaction products, the reaction mechanism is shown in Figures 5, 6. As shown in Figure 5, the carbon fluorine bond connected to aryl and alkenyl groups has high activity, and is the first to undergo nucleophilic reaction with KOH. There are two possible mechanisms for the reaction of carbon fluorine bond reaction connected to the alkenyl group. One is that the hydroxyl group attacks the carbon atom directly, resulting in the removal of the F ion to form an alcohol. The unstable enol is then readily converted into a carbonyl group (Figure 5A). Another consideration is that the carbon-carbon double bond undergoes methanol addition, and the introduction of an -OH group allows the F ion to leave easily while simultaneously accepting an OH^- ion (Figure 5B). The carbon fluorine bond connected to the aryl group can react only in the manner shown in Figure 5C.

There are two possible reaction mechanisms involving electron transfer. The carbon fluorine bond obtains two electrons by electroreduction, which directly generates fluorine ions and carbon anions, and carbon anions capture hydrogen ions, (Figure 6A). It is also possible that a single electron transfers to the F atom, which then becomes the F ion to leave. Hydroxide is then combined with an unstable carbon atom, losing fluorine and releasing an electron, in which electrons act as a catalyst (Figure 6B). Considering the products, OFG1.17 also contains hydrocarbons, and the carbon content of the products increases after the reaction, which proves that an addition reaction has occurred between methanol and the carbon-carbon double bonds.

As shown in Figure 7, when the carbon fluorine bond connected to the aryl or alkenyl group reacts completely, the carbon fluorine bond attached to the carbon atom linked with the alkenyl or aryl group undergoes a nucleophilic reaction with KOH. Nucleophilic reactions may also occur under electron transfer (Figure 6). The final reaction is the most inactive alkyl carbon fluorine bond and its mechanism is similar to that mentioned previously. In addition, the carbon fluorine

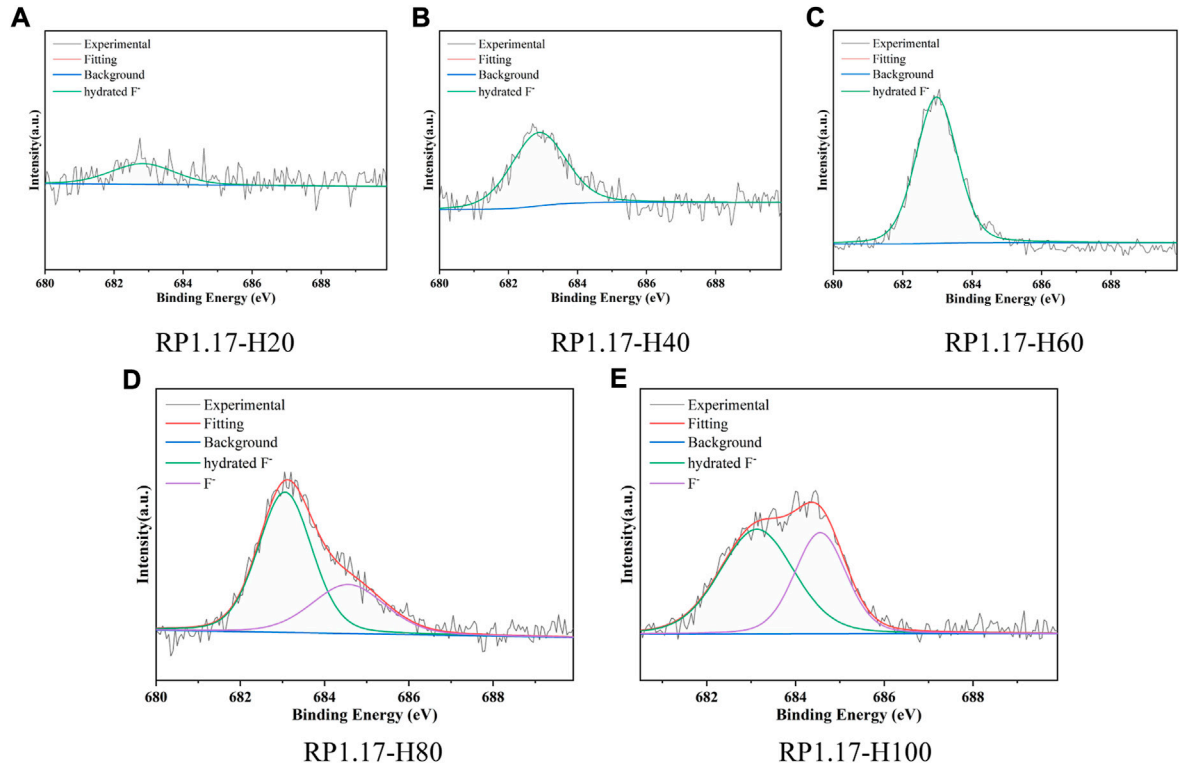

FIGURE 4
High-resolution F1s spectra of RP1.17-H: H20(20°C), H40(40°C), H60(60°C), H80(80°C), and H100(100°C).

TABLE 4 F content of all products of $CF_{1.17}$ before and after the modification.

FGi (mg)	F Content (mg)	OFG	F Content (mg)	RP	F Ion content (mg)
500	325	OFG1.17-E2	315	RP1.17-E2	4.4
500	325	OFG1.17-E5	286.5	RP1.17-E5	40.5
500	325	OFG1.17-E00	13.8	RP1.17-E00	286.3
500	325	OFG1.17-E01	52.8	RP1.17-E01	238.0
500	325	OFG1.17-H20	306	RP1.17-H20	10.6
500	325	OFG1.17-H40	289	RP1.17-H40	22.6
500	325	OFG1.17-H60	105	RP1.17-H60	218.4
500	325	OFG1.17-H80	21.7	RP1.17-H80	299.1
500	325	OFG1.17-H100	10.6	RP1.17-H100	311.1

bonds in $-CF_2$ and $-CF_3$ undergo nucleophilic substitution, resulting in the formation of geminal diol structures, which are extremely unstable and very easy to dehydrate into aldehydes or ketones, as shown in Figure 8. Therefore, when $-CF_2$ and $-CF_3$ are completely substituted, they become ketone and carboxyl groups, respectively, explaining the source of carbonyl groups in OFG. In addition, the existing carbon-carbon double bond theoretically reacts with the weakly nucleophilic methanol.

As shown in the above mechanism, with the increase in electrolysis time, the carbon fluorine bond gradually reacts with KOH according to its reactive activity, and then the F atom is replaced. However, according to the XPS results, not all carbon fluorine bonds are converted into carbon oxygen bonds. One

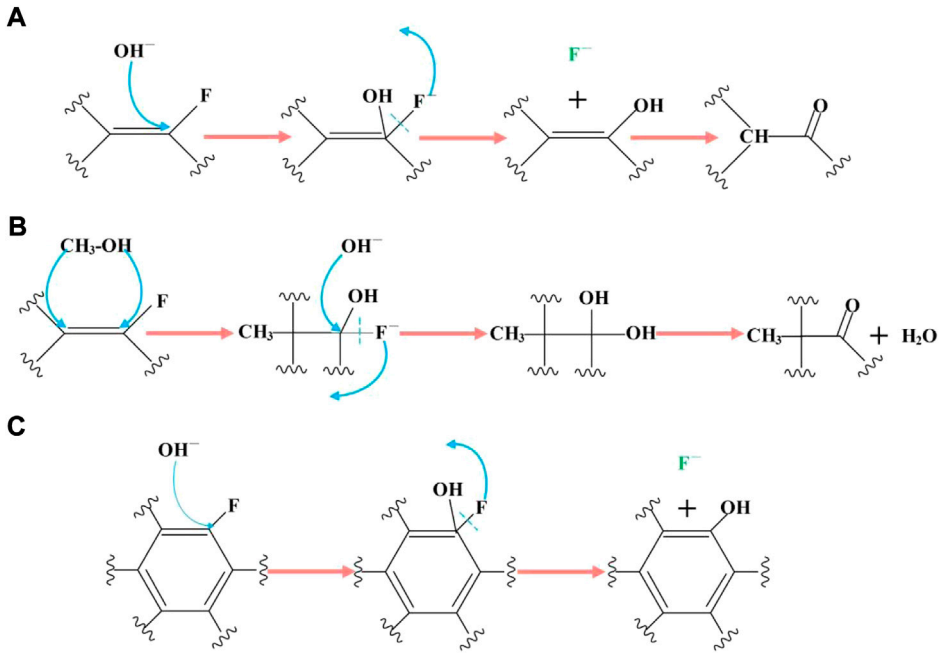

FIGURE 5
Nucleophilic reaction mechanism between KOH and C-F bond.

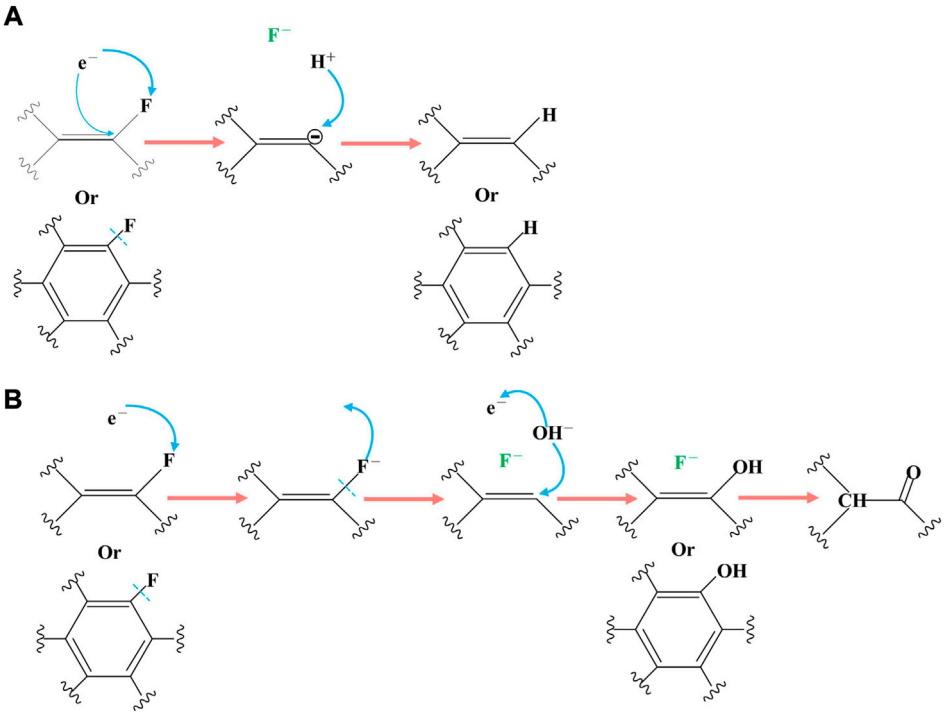

FIGURE 6
Nucleophilic reaction mechanism under electron transfer conditions.

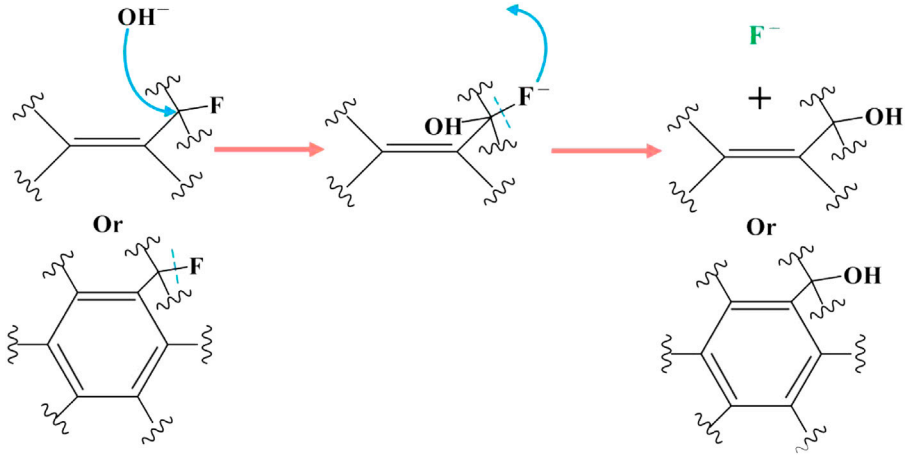

FIGURE 7
Nucleophilic reaction mechanism between KOH and subactive C-F bond.

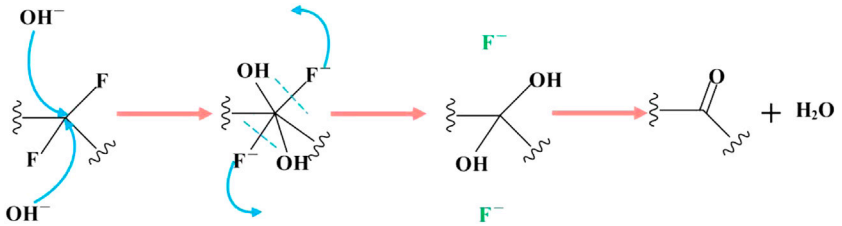

FIGURE 8
Carbonyl formation mechanism in OFG1.17 products.

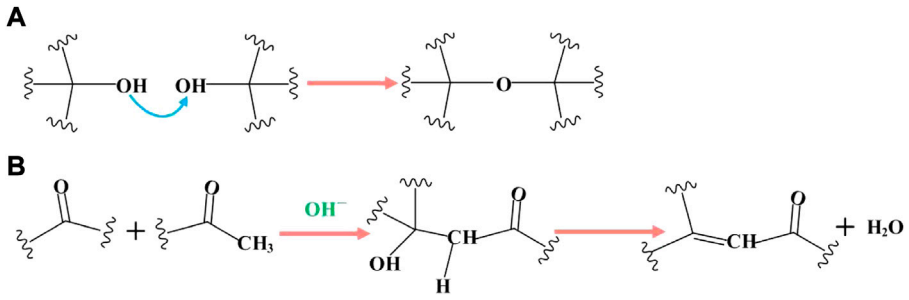

FIGURE 9
OFG deoxidation mechanism under strong alkalinity.

reason is that with the increase in time, the carbon oxygen bond may be partially reduced to a carbon-carbon double bond by the cathode, but this should only account for a very small percentage of bond formed. Another reason is that the dehydration polymerization of adjacent hydroxyl groups may occur in the presence of a large number of hydroxyl groups (Figure 9A), and the aldol condensation reaction may also occur after the addition of methanol, which forms a carbon-carbon double bond

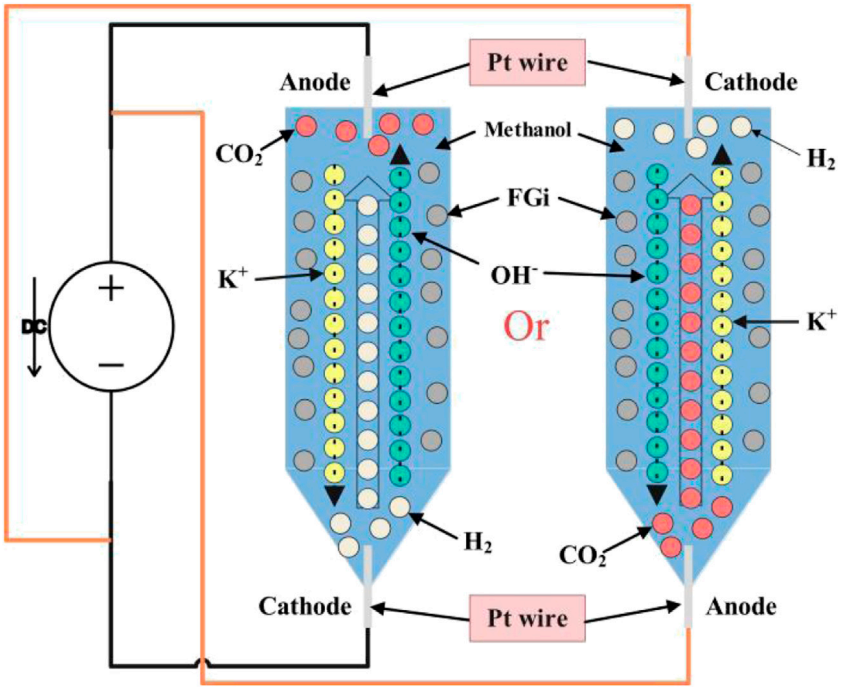

FIGURE 10
Principle display of the electrolysis of KOH methanol solution.

(Figure 9B). Carbon oxygen bonds can also be deoxidized under strong alkalinity (Dimiev et al., 2012): the attack of hydroxyl ions on the carbonyl group leads to the fracture of carbon-carbon bonds and the formation of carboxyl groups. Subsequent decarboxylation forms the structure shown in the literature, releasing carbon dioxide. This fracture, as well as the oxidation fracture of unsaturated carbon bonds in $CF_{1.17}$, also explains the presence of GO fragments in the filtrate.

As shown in Supplementary Table S1, the carbon oxygen bond contents of OFG1.17-E00 and OFG1.17-E01 are similar, but the carbon fluorine bond content is quite different, and the only difference between them is the anode location. This can be explained by the difference in the direction of the ion current and products due to the different anode positions. When the anode is at the bottom, it generates CO_2 gas flow adjacent to it, driving FGi to move upward against the flow of OH^- ions (Figure 10). Increasing the contact between the two reactants increases the probability of a nucleophilic reaction. However, OH^- ions react with CO_2 more easily, rather than undergoing a nucleophilic reaction with FGi, so OFG1.17-E01 can maintain a high fluorine content. When the anode is at the top, CO_2 directly overflows, and the flow of H_2 drives FGi and OH^- ions to move in the same direction; thus, OH^- ions cannot react with CO_2, increasing the probability of nucleophilic reaction. Besides avoiding the reaction of KOH with CO_2, the activation of carbon fluorine bonds by electron transfer further promotes the nucleophilic reaction between KOH and the isolated saturated carbon fluorine bonds. These reasons may explain the difference between OFG1.17-E00 and OFG1.17-E01. In addition, OFG1.17 has no C=O bond and a few possible O-C=O bonds in an electro-oxidative environment, indicating that a 60 V DC cannot oxidize $CF_{1.17}$. Strong alkalis such as NaOH and KOH can suppress the oxidation reaction (Alshamkhani Maher et al., 2021) and the FGi powder moves with the boiling of the solution and the movement of the air flow in it.

The reaction mechanism of KOH heating method is similar to that of the KOH methanol electrochemical method; however, there is no nucleophilic reaction caused by electron transfer. The possible mechanism is shown in Figures 5, 7, 8. The reaction occurs based on the reaction reactivity of the carbon fluorine bond. In addition, the full substitution of $-CF_2$ and $-CF_3$, respectively results in the formation of ketone and carboxyl groups, respectively. As shown in Figure 9, it is deoxidized under strong alkali condition, resulting in the reduction of the carbon oxygen bonds and the fracture of the carbon skeleton. The decrease in temperature results in a decrease of carbon fluorine bond reaction reactivity from OFG1.17-H100 to OFG1.17-H20, along with an increase in carbon fluorine bonds and a decrease in F ions.

According to the previous analysis, KOH can react with the carbon fluorine bond with higher reactivity, and the basic principle is similar, although in different places. The

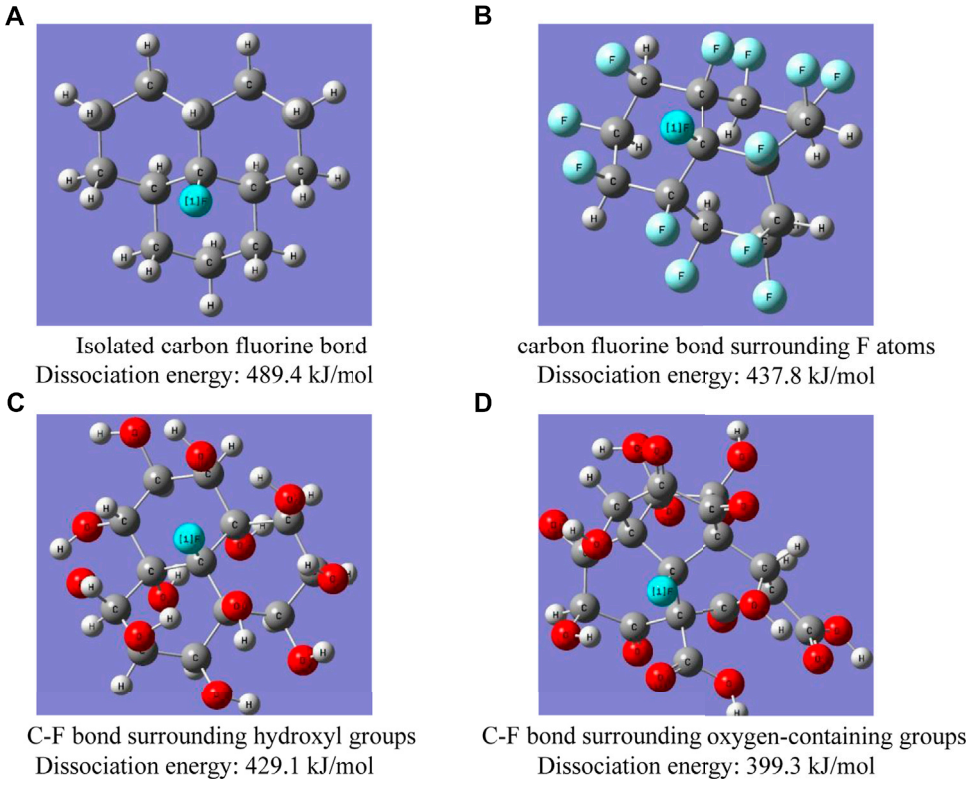

FIGURE 11
Schematic structure of the carbon fluorine bond at different positions.

electrochemical method using the bottom anode can destroy most of the carbon fluorine bonds of $CF_{1.17}$, leaving some retained. $CF_{0.95}$ can retain more carbon fluorine bonds under the same conditions, while $CF_{0.46}$ is in the middle. The same law still exists in the modification of FGi using the KOH ethanol heating method, leaving some carbon fluorine bonds that cannot react with KOH. Among the electrochemical methods, only when the anode is on the top can these carbon fluorine bonds react *via* electron transfer activation.

In order to confirm that the dissociation energy of the isolated carbon fluorine bond is high and difficult to be activated to participate in the reaction, the following theoretical simulation calculation is carried out for the different positions of the carbon fluorine bond. The methods are as follows: using the DFT method at the level of B3LYP (Lee et al., 1988; Perdew and Wang, 1989)/6-311G (d, p) (Ditchfield et al., 1971), the whole structure of different carbon fluorine bonds is optimized. The vibration analysis confirms that there is no virtual frequency at the equilibrium point. The single-point energies of the entire structure, the fluorine atom fragments and the remaining structures are then calculated. The carbon fluorine bond dissociation energy can be obtained by subtracting the single-point energy of the whole structure from the sum of the single-point energies of both fragments. All the calculations are performed on the Dawning workstation using the Gaussian 09 package (Gaussian et al., 2009).

Four different structures are constructed, and their carbon fluorine bonds are located at different positions. Figure 11A shows the isolated carbon fluorine bond structure. Figure 11B shows the carbon fluorine bond structure surrounded by other carbon fluorine bonds, which is similar to the carbon fluorine bond in FGi with complete fluorination. Figure 11C illustrates the carbon fluorine bond surrounded by the hydroxy group, assuming that the carbon fluorine bond undergoes a complete nucleophilic reaction with KOH, and Figure 11D shows the carbon fluorine bond surrounded by oxygen-containing groups (e.g., hydroxy, carbonyl, carboxyl). The dissociation energy of the isolated C-F bond, the C-F bond surrounded by F atoms, the C-F bond surrounded by hydroxyl groups and the C-F bond surrounded by oxygen-containing groups are calculated as 489.4, 437.8, 429.1, and 399.3 kJ/mol, respectively. The dissociation energy of the isolated carbon fluorine bond is much higher than that of the carbon fluorine bond surrounded by other electronegative groups. When C-O bonds, C=O bonds and O-C=O bonds replace the carbon fluorine bonds around the carbon fluorine bonds, the

dissociation energy of the carbon fluorine bond is at its lowest. Once the carbon fluorine bonds are replaced by oxygen-containing groups, the dissociation energy of the carbon fluorine bonds decreases, thereby accelerating the reaction of the carbon fluorine bonds. Due to its highest dissociation energy and lowest reactivity, the isolated carbon fluorine bond can only react under the condition of electron catalytic transfer.

The residual carbon fluorine bond of OFG0.95 has the highest dissociation energy, followed by OFG0.46, and OFG1.17 is the least. The reason is that $CF_{1.17}$ with complete fluorination owns the least isolated carbon fluorine bond, and the carbon fluorine bond of $CF_{0.46}$ with incomplete fluorination is concentrated on the edge and defect, resulting in fewer internal isolated carbon fluorine bonds, whereas $CF_{0.95}$, fluorinated completely at the edge and defect and incompletely fluorinated in the interior, has more isolated carbon fluorine bond structures in its internal structure. The isolated carbon fluorine bond is unlikely to participate in the reaction due to its high dissociation energy and weak reactivity. Electronegative groups can reduce the dissociation energy of the carbon fluorine bond and increase its reactivity when they are located around the carbon fluorine bond.

4 Conclusion

The modification of $CF_{1.17}$ by KOH caused the F ion content in the residual product of the reaction to increase with the electrochemical reaction time or heating temperature, as the reaction is nucleophilic, while the carbon fluorine bond content in the corresponding OFG gradually decreases. After complete electrolysis, the oxygen content of the OFG is approximately 15 at%, with the position of the anode greatly affecting its fluorine content of the OFG. When the anode is at the bottom, there are still some carbon fluorine bonds and the F content is 11.4 at %, but moving the anode to the top causes the carbon fluorine bonds to almost completely disappear and the F content decreases to only 1.7 at%. The reason is that CO_2 generated at the anode reacts more easily with KOH than with FGi, thus preventing the nucleophilic reaction between KOH and FGi. Furthermore, electron transfer greatly promotes the activation of the carbon fluorine bond, resulting in a complete reaction. FGi undergoes a nucleophilic reaction with KOH according to its carbon fluorine bond reaction reactivity, replacing the F atoms are then. The carbon fluorine bond connected to the aryl or alkenyl group reacts first, followed by the carbon fluorine bond attached to the carbon atom linked with the alkenyl or aryl group, and the isolated carbon fluorine bond is the last to react. The reaction mechanism of the KOH heating method is similar except for the promotion of the electron transfer.

OFG0.95 contains the most residual carbon fluorine bonds under the same conditions, followed by OFG0.46, and OFG1.17 has the least. The reason is that the edges and defects of $CF_{0.95}$ are completely fluorinated, but the internal fluorination is incomplete, which leads to a more isolated carbon fluorine bond structure. According to the theoretical simulation calculations, the isolated carbon fluorine bond owns the highest dissociation energy and the lowest reactivity, but the introduction of electronegative groups can decrease its dissociation energy and increase its reactivity.

Data availability statement

The original contributions presented in the study are included in the article/Supplementary Material, further inquiries can be directed to the corresponding authors.

Author contributions

HL wrote the main manuscript text. GH and SB carried out the experimental design and guidance. ZL assisted in completing the experimental analysis. XY and WL checked and revised the article. YS prepared Figures 10, 11. All authors reviewed the manuscript.

Funding

This research was supported by the Youth Foundation Program of Xi'an Research Institute of High-Tech (Program No.2020QNJJ009).

Conflict of interest

The authors declare that the research was conducted in the absence of any commercial or financial relationships that could be construed as a potential conflict of interest.

Publisher's note

Supplementary material

The Supplementary Material for this article can be found online at: https://www.frontiersin.org/articles/10.3389/fmats.2022.999753/full#supplementary-material

References

Alshamkhani Maher, -T., Lee-Keat, T., Lutfi-Kurnianditia, P., Mohamed, A. R., Lahijani, P., and Mohammadi, M. (2021). Effect of graphite exfoliation routes on the properties of exfoliated graphene and its photocatalytic applications. *J. Environ. Chem. Eng.* 9 (6), 106506. doi:10.1016/j.jece.2021.106506

Andrieux, C. P., Combellas, C., Kanoufi, F., Saveant, J. M., and Thiebault, A. (1997). Dynamics of bond breaking in ion radicals. Mechanisms and reactivity in the reductive cleavage of Carbon−Fluorine bonds of fluoromethylarenes. *J. Am. Chem. Soc.* 119 (40), 9527–9540. doi:10.1021/ja971094o

Borse, R. A., Kale, M. B., Sonawane, S. H., and Wang, Y. (2022). Fluorographene and its composites: Fundamentals, electrophysical properties, DFT studies, and advanced applications. *Adv. Funct. Mat.* 32, 2202570. doi:10.1002/adfm.202202570

Bosch-navarro, C., Walker, M., Wilson, N-R., and Rourke, J. P. (2015). Covalent modification of exfoliated fluorographite with nitrogen functionalities. *J. Mat. Chem. C Mat.* 3 (29), 7627–7631. doi:10.1039/c5tc01633a

Bourlinos Athanasios, -B., Vasilios, G., Radek, Z., Jancik, D., Karakassides, M. A., Stassinopoulos, A., et al. (2008). Reaction of graphite fluoride with NaOH–KOH eutectic. *J. Fluor. Chem.* 129 (8), 720–724. doi:10.1016/j.jfluchem.2008.05.020

Chen, X., Fan, K., Liu, Y., Li, Y., Liu, X., Feng, W., et al. (2021). Recent advances in fluorinated graphene from synthesis to applications: Critical review on functional chemistry and structure engineering. *Adv. Mater.* 34, 2101665. doi:10.1002/adma.202101665

Chronopoulos Demetrios, -D., Aristides, B., Petr, L., Pykal, M., Cepe, K., Zboril, R., et al. (2017). High-yield alkylation and arylation of graphene via grignard reaction with fluorographene. *Chem. Mat.* 29 (3), 926–930. doi:10.1021/acs.chemmater.6b05040

Dimiev, A. M., Alemany, L. B., and Tour, J. M. (2012). Graphene oxide. Origin of acidity, its instability in water, and a new dynamic structural model. *ACS Nano* 7 (1), 576–588. doi:10.1021/nn3047378

Ditchfield, R., Hehre, W. J., and Pople, J. A. (1971). Self-consistent molecular-orbital methods. IX. An extended Gaussian-type basis for molecular-orbital studies of organic molecules. *J. Chem. Phys.* 54 (2), 724–728. doi:10.1063/1.1674902

Fan, Li, Wei, Weili, and Gao, Die (2017). The adsorption behavior and mechanism of perfluorochemicals on oxidized fluorinated graphene sheets supported on silica[J]. *Anal. Methods* 9 (47), 6645–6652.

Gaussian, R. A., Frisch, M. J., Trucks, G. W., Schlegel, H. B., Ge, S., Cheeseman, M. A., et al. (2009). Gaussian[J], 121. Wallingford Ct: Inc., 150–166.

Gong, P., Ji, S., Wang, J., Dai, D., Wang, F., Tian, M., et al. (2018). Fluorescence-switchable ultrasmall fluorinated graphene oxide with high near-infrared absorption for controlled and targeted drug delivery. *Chem. Eng. J.* 348, 438–446. doi:10.1016/j.cej.2018.04.193

Gong, P., Yang, Z., Hong, W., Wang, Z., Hou, K., Wang, J., et al. (2015). To lose is to gain: Effective synthesis of water-soluble graphene fluoroxide quantum dots by sacrificing certain fluorine atoms from exfoliated fluorinated graphene. *Carbon* 83, 152–161. doi:10.1016/j.carbon.2014.11.027

Guguloth, L., Shekar, P. V. R., Channu, V. S. R., and Kumari, K. (2021). Effect of reduced fluorinated graphene oxide as ternary component on synergistically boosting the performance of polymer bulk heterojunction solar cells. *Sol. Energy* 225, 259–265. doi:10.1016/j.solener.2021.07.020

He, P., Cao, M. S., Shu, J. C., Cai, Y. Z., Wang, X. X., Zhao, Q. L., et al. (2019). Atomic layer tailoring titanium carbide MXene to tune transport and polarization for utilization of electromagnetic energy beyond solar and chemical energy. *ACS Appl. Mat. Interfaces* 11 (13), 12535–12543. doi:10.1021/acsami.9b00593

He, P., Liu, Z. Y., Mao, G. B., Liu, Q., Zheng, M. J., Zuo, R. Z., et al. (2022). MXene films: Toward high-performance electromagnetic interference shielding and supercapacitor electrode. *Compos. Part A Appl. Sci. Manuf.* 157, 106935. doi:10.1016/j.compositesa.2022.106935

Hou, K., Gong, P., Wang, J., Yang, Z., Wang, Z., and Yang, S. (2014). Structural and tribological characterization of fluorinated graphene with various fluorine contents prepared by liquid-phase exfoliation. *RSC Adv.* 4 (100), 56543–56551. doi:10.1039/c4ra10313k

Jahanshahi, M., Kowsari, E., Haddadi-Asl, V., Khoobi, M., Bazri, B., Aryafard, M., et al. (2020). An innovative and eco-friendly modality for synthesis of highly fluorinated graphene by an acidic ionic liquid: Making of an efficacious vehicle for anti-cancer drug delivery. *Appl. Surf. Sci.* 515, 146071. doi:10.1016/j.apsusc.2020.146071

Kaczmarek, Ł., Balik, M., Warga, T., Acznik, I., Lota, K., Miszczak, S., et al. (2021). Functionalization mechanism of reduced graphene oxide flakes with BF_3·THF and its influence on interaction with Li^+ ions in lithium-ion batteries. *Materials* 14 (3), 679. doi:10.3390/ma14030679

Kouloumpis, A., Chronopoulos, D. D., Potsi, G., Pykal, M., Vlcek, J., Scheibe, M., et al. (2020). One-step synthesis of janus fluorographene derivatives. *Chem. Eur. J.* 26 (29), 6518–6524. doi:10.1002/chem.201905866

Lee, C., Yang, W., and Parr, R. G. (1988). Development of the Colle-Salvetti correlation-energy formula into a functional of the electron density. *Phys. Rev. B* 37 (2), 785–789. doi:10.1103/physrevb.37.785

Li, B., He, T., and Wang, Z. (2016). Chemical reactivity of C-F bonds attached to graphene with diamines depending on their nature and location.[J]. *Phys. Chem. Chem. Phys.* 18 (26), 505–17495.

Li, H., Bi, S., and Yuan, X. (2022). Oxidation modification of fluorinated graphite and its reaction mechanism[J]. *Bull. Mater. Sci.* 45 (2), 1–12.

Liang, X., Lao, M., Pan, D., Liang, S., Huang, D., Zhou, W., et al. (2017). Facile synthesis and spectroscopic characterization of fluorinated graphene with tunable C/F ratio via Zn reduction. *Appl. Surf. Sci.* 400 (1), 339–346. doi:10.1016/j.apsusc.2016.12.211

Ma, L., Li, Z., Jia, W., Hou, K., Wang, J., and Yang, S. (2021). Microwave-assisted synthesis of hydroxyl modified fluorinated graphene with high fluorine content and its high load-bearing capacity as water lubricant additive for ceramic/steel contact. *Colloids Surfaces A Physicochem. Eng. Aspects* 610, 125931. doi:10.1016/j.colsurfa.2020.125931

Matsuo, Y., Hirata, S., and Dubois, M. (2016). Electrochemical oxidation of graphite in aqueous hydrofluoric acid solution at high current densities. *J. Fluor. Chem.* 185, 36–41. doi:10.1016/j.jfluchem.2016.01.015

Matúš, Dubecký, Eva, Otyepková, and Petr, Lazar (2015). Reactivity of fluorographene: A facile way toward graphene derivatives[J]. *J. Phys. Chem. Lett.* 6 (8), 1430–1434.

Menia, S., Tebibel, H., Lassouane, F., Khellaf, A., and Nouicer, I. (2017). Hydrogen production by methanol aqueous electrolysis using photovoltaic energy: Algerian potential. *Int. J. Hydrogen Energy* 42 (13), 8661–8669. doi:10.1016/j.ijhydene.2016.11.178

Perdew, J. P., and Wang, Y. (1989). Accurate and simple density functional for the electronic exchange energy: Generalized gradient approximation. *Phys. Rev. B* 33 (12), 8800–8802. doi:10.1103/physrevb.33.8800

Razaghi, M., Ramazani, A., Khoobi, M., Mortezazadeh, T., Aksoy, E. A., and Kucukkilinc, T. T. (2020). Highly fluorinated graphene oxide nanosheets for anticancer linoleic-curcumin conjugate delivery and T_2-weighted magnetic resonance imaging: *In vitro* and *in vivo* studies[J]. *J. Drug Deliv. Sci. Technol.* 60, 101967. doi:10.1016/j.jddst.2020.101967

Robinson, Jeremy T., Burgess, James S., Junkermeier, Chad E., Badescu, S. C., Reinecke, T. L., Perkins, F. K., et al. (2010). Properties of fluorinated graphene films. *Nano Lett.* 10 (8), 3001–3005. doi:10.1021/nl101437p

Siedle, A. R., Losovyj, Y., Karty, J. A., Chen, D., Chatterjee, K., Carta, V., et al. (2021). C–F bond activation in the solid state: Functionalization of carbon through reactions of graphite fluoride with amines. *J. Phys. Chem. C* 125 (19), 10326–10333. doi:10.1021/acs.jpcc.1c00734

Sim, Y., Surendran, S., Cha, H., Choi, H., Je, M., Yoo, S., et al. (2022). Fluorine-doped graphene oxide prepared by direct plasma treatment for supercapacitor application. *Chem. Eng. J.* 428, 132086. doi:10.1016/j.cej.2021.132086

Veronika, U., Kateřina, H., and Bourlinos Athanasios, -B. (2015). Thiofluorographene-hydrophilic graphene derivative with semiconducting and genosensing properties[J]. *Adv. Mater.* 27 (14), 2305–2310.

Whitener, K-E., Jr, Stine, R., Robinson, J-T., and Sheehan, P. E. (2015). Graphene as electrophile: Reactions of graphene fluoride. *J. Phys. Chem. C* 119 (19), 10507–10512. doi:10.1021/acs.jpcc.5b02730

Xu, Y., Di, M., Wang, Y., Fu, L., Du, Y., and Tang, N. (2021). Structure, bandgap and photoluminescence of fluorinated reduced graphene oxide. *Diam. Relat. Mater.* 114, 108342. doi:10.1016/j.diamond.2021.108342

Yamamoto, H., Matsumoto, K., Matsuo, Y., Sato, Y., and Hagiwara, R. (2020). Deoxofluorination of graphite oxide with sulfur tetrafluoride. *Dalton Trans.* 49 (1), 47–56. doi:10.1039/c9dt03782a

Ye, X., Ma, L., Yang, Z., Wang, J., Wang, H., and Yang, S. (2016). Covalent functionalization of fluorinated graphene and subsequent application as water-based lubricant additive. *ACS Appl. Mat. Interfaces* 8 (11), 7483–7488. doi:10.1021/acsami.5b10579

Yeon-Hoo, Kim, Soo-Park, Ji, and You-Rim, Choi (2017). Chemically fluorinated graphene oxide for room temperature ammonia detection at ppb levels[J]. *J. Mater. Chem. A* 5 (36), 19116–19125.

Zhang, G., Zhou, K., Xu, R., Chen, H., Ma, X., Zhang, B., et al. (2016). An alternative pathway to water soluble functionalized graphene from the defluorination of graphite fluoride. *Carbon* 96, 1022–1027. doi:10.1016/j.carbon.2015.10.020

Zhang, M., Han, C., and Cao, W. Q. (2021). A nano-micro engineering nanofiber for electromagnetic absorber, green shielding and sensor[J]. *Nano-micro Lett.* 13 (1), 1–12.

Zhao, S., Dou, B., Duan, S., Lin, X., Zhang, Y., Emori, W., et al. (2021). Influence of fluorinated graphene-modified epoxy coatings on the corrosion behaviour of 2024 aluminium alloy. *RSC Adv.* 11 (29), 17558–17573. doi:10.1039/d1ra01870a

Zhu, W., Wu, C., Chang, Y., Cheng, H., and Yu, C. (2019). Solvent-free preparation of hydrophilic fluorinated graphene oxide modified with amino-groups. *Mater. Lett.* 237, 1–4. doi:10.1016/j.matlet.2018.09.174